# Towards Atomistic Resolution Structure of Phosphatidylcholine Headgroup and Glycerol Backbone at Different Ambient Conditions[†]

Alexandru Botan,[‡] Fernando Favela-Rosales,[¶] Patrick F. J. Fuchs,[§] Matti Javanainen,[‖] Matej Kanduč,[⊥] Waldemar Kulig,[‖] Antti Lamberg,[#] Claire Loison,[‡] Alexander Lyubartsev,[@] Markus S. Miettinen,[△] Luca Monticelli,[∇] Jukka Määttä,[††] O. H. Samuli Ollila,[*,††] Marius Retegan,[‡‡] Tomasz Rog,[‖] Hubert Santuz,[¶¶,§§,‖‖,⊥⊥] and Joona Tynkkynen[‖]

*Institut Lumière Matière, UMR5306 Université Lyon 1-CNRS, Université de Lyon 69622 Villeurbanne, France, Departamento de Física, Centro de Investigación y de Estudios Avanzados del IPN, Apartado Postal 14-740, 07000 México D.F., México, Institut Jacques Monod, CNRS, Université Paris Diderot, Sorbonne Paris Cité, Paris, France, Department of Physics, Tampere University of Technology, Tampere, Finland, Fachbereich Physik, Freie Universitat Berlin, Berlin, Germany, Department of Chemical Engineering, Kyoto University, Kyoto, Japan, Division of Physical Chemistry, Department of Materials and Environmental Chemistry, Stockholm University, S-106 91 Stockholm, SWEDEN, Fachbereich Physik, Freie Universität Berlin, Berlin, Germany, Institut de Biologie et Chimie des Protéines (IBCP), CNRS UMR 5086, Lyon, France, Aalto University, Espoo, Finland, Max Planck Institute for Chemical Energy Conversion, Mulheim an der Ruhr, Germany, INSERM, UMR_S 1134, DSIMB, Paris, France, Université Paris Diderot, Sorbonne Paris Cité, UMR_S 1134, Paris, France, Institut National de la Transfusion Sanguine (INTS), Paris, France, and Laboratoire d'Excellence GR-Ex, Paris, France*

E-mail: samuli.ollila@aalto.fi.

**Abstract**

Phospholipids are essential building blocks of biological membranes. Despite of vast amount of very accurate experimental data, the atomistic resolution structures sampled by the glycerol backbone and choline headgroup in phoshatidylcholine bilayers are not known. Atomistic resolution molecular dynamics simulations have the potential to resolve the structures, and to give an arrestingly intuitive interpretation of the experimental data—but only if the simulations reproduce the data within experimental accuracy. In the present work, we simulated phosphatidylcholine (PC) lipid bilayers with 13 different atomistic models, and compared simulations with NMR experiments in terms of the highly structurally sensitive C–H bond vector order parameters. Focusing on the glycerol backbone and choline headgroups, we showed that the order parameter comparison can be used to judge the atomistic resolution structural accuracy of the models. Accurate models, in turn, allow molecular dynamics simulations to be used as an interpretation tool that translates these NMR data into a dynamic three dimensional representation of biomolecules in biologically relevant conditions. In addition to lipid bilayers in fully hydrated conditions, we reviewed previous experimental data for dehydrated bilayers and cholesterol-containing bilayers, and interpreted them with simulations. Although none of the existing models reached experimental accuracy, by critically comparing them we were able to distill relevant chemical information: (1) increase of choline

[†]Publication about results presented in the NMRlipids project

[*]To whom correspondence should be addressed
[‡]Lyon CNRS
[¶]Mexico
[§]CNRS Paris
[‖]Tampere University of Technology
[⊥]Freie Universität Berlin
[#]Kyoto University
[@]Stockholm University
[△]Freie Universität Berlin
[▽]IBCP
[††]Aalto University
[‡‡]Max Planck
[¶¶]INSERM
[§§]Diderot
[‖‖]INTS
[⊥⊥]Labex

order parameters indicates the P–N vector tilting more parallel to the membrane, and (2) cholesterol induces only minor changes to the PC (glycerol backbone) structure. This work has been done as a fully open collaboration, using `nmrlipids.blogspot.fi` as a communication platform; all the scientific contributions were made publicly on this blog. During the open research process, the repository holding our simulation trajectories and files (`https://zenodo.org/collection/user-nmrlipids`) has become the most extensive publicly available collection of molecular dynamics simulation trajectories of lipid bilayers.

## Keywords

American Chemical Society, LaTeX

## Introduction

Phospholipids containing various polar headgroups and acyl chains are essential building blocks of biological membranes. Lamellar phospholipid bilayer structures have been widely studied with various experimental and theoretical techniques as a simple model for cellular membranes.[1–8] Phospholipid molecules are composed of hydrophobic acyl chains connected by a glycerol backbone to a hydrophilic headgroup; see Fig. 1 for the structure of 1-palmitoyl-2-oleoylphosphatidylcholine (POPC). The behaviour of the acyl chains in a lipid bilayer is relatively well understood.[1–5,8,9] The conformations sampled by the glycerol backbone and choline in a fluid bilayer are, however, not fully resolved as even the most accurate scattering and Nuclear Magnetic Resonance (NMR) techniques give only a set of values that the structure has to fulfill, but there is no unique way to derive the actual structure from them.[9–18] Some structural details have been extracted from crystal structures, $^{1}$H NMR studies, and Raman spectroscopy,[19–25] but general consensus concerning the structures sampled in the fluid state has not been reached.[9–18,24,25] Importantly, the structural parameters for the glycerol backbone are similar for various biologically relevant lipid species (phosphatidylcholine (PC), phosphatidylethanolamine (PE) and phosphatidylglycerol (PG)) in various environments,[26] and the structural parameters for the choline headgroup are similar in model membranes and real cells (mouse fibroblast L-M cell).[27] Thus, resolving the PC-lipid glycerol and choline structures would be useful for understanding a wide range of different biological membranes.

Classical atomistic molecular dynamics simulations have been widely used to study lipid bilayers.[2–7] As these models provide an atomistic resolution description of the whole lipid molecule, they have the potential to solve the glycerol backbone and headgroup structures. The experimental C–H bond order parameters (routinely compared between experiments and simulations for the acyl chains[2–6]) are also known for the glycerol backbone ($g_1$, $g_2$, and $g_3$) and choline ($\alpha$ and $\beta$) segments (see Fig. 1 for definitions) and are among the main parameters used in attempts to derive lipid structures from experimental data.[10–13,15,16,18] Notably, the structures sampled in a simulation that reproduces these parameters will automatically comprise an interpretation of the experiments. In other words, such simulations can be considered as an accurate atomistic resolution description of the behavior of lipid molecules in a bilayer.

Only a few studies[28–37] have compared the glycerol backbone and choline headgroup order parameters between simulations and experiments. The main reason probably is that the existing experimental data for the glycerol backbone and choline headgroups are scattered over many publications and published in a format that is difficult to understand without some NMR expertise. In addition to the order parameters, dihedral angles for the glycerol backbone and headgroup estimated from experiments,[28,38–42] $^{31}$P chemical shift anisotropy[36] and $^{31}$P-$^{13}$C dipolar couplings[43] have been used to assess the quality of a simulation model.

In this work, we first review the most relevant experimental data for the glycerol backbone and choline headgroup order parameters in a phosphatidylcholine lipid bilayer. Then the available atomistic resolution lipid models are carefully compared to the experimental data.

The comparison reveals that the CHARMM36,[31] GAFFlipid,[33] and MacRog[37] models have the most realistic glycerol backbone and choline structures. We also compare the glycerol backbone and choline structures between the most often used (Berger-based) lipid model[44] and the best performing models, to demonstrate that by using the order parameters we can distinguish the more reasonable structures from the less reasonable ones. However, none of the current models is accurate enough to properly resolve the atomistic resolution structures.

In addition to fully hydrated single component lipid bilayers, the glycerol backbone and choline order parameters have been measured under a large number of changing conditions: hydration level,[45–47] cholesterol content,[35,48] ion concentration,[49–53] temperature,[54] charged lipid content,[52,53] charged surfactant content,[55] drug molecule concentration,[30,56,57] and protein content[58,59] (listing only the publications most relevant for this work and the pioneering studies). Existence of these data allows the comparison of structural responses to varying conditions between simulations and experiments, in other words, validation of the simulation models and interpretation of the original experiments. Here we demonstrate the power of this approach in understanding the behaviour of a bilayer as a function of hydration level and cholesterol content. Choline headgroup order parameters as function of ion concentration, and their relation to the ion binding affinity, are discussed elsewhere.[60]

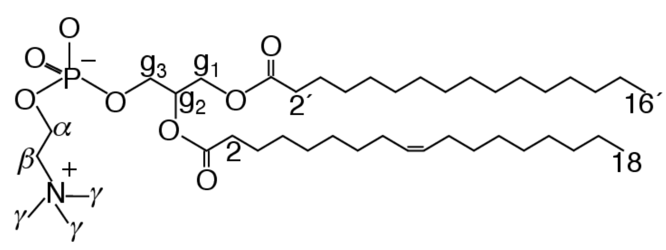


Figure 1: Chemical structure of 1-palmitoyl-2-oleoylphosphatidylcholine (POPC).

# Methods

## Open collaboration

This work has been done as a fully open collaboration, using the `nmrlipids.blogspot.fi` blog[61] as a communication platform. Our approach is inspired by the Polymath project,[62] however there are some essential differences. We started by publishing a manuscript[63] discussing the glycerol backbone and choline structures in a Berger-based model (the most used molecular dynamics simulation model for lipid bilayers). Simultaneously, we presented an open invitation for further contributions and discussion on the blog. All the scientific contributions were made publicly through the blog. Every contributor was offered coauthorship according to the guidelines defined in the beginning of the project;[64] the acceptance of the offer was based on authors' self-assesment of their scientific contribution. These contributions are summarized in the Supporting Information.

Almost all simulation data, including input files for reproduction and trajectories for further analysis, are collected on our CERN-hosted Zenodo file repository (`https://zenodo.org/collection/user-nmrlipids`). Thus, in addition to the main topic of this manuscript, we present the most extensive publicly available collection of simulation trajectories for lipid bilayers, opening up numerous possiblities for different analyses with much less effort than previously required. Further information, such as scripts, figures, and manuscript text files, are available through our GitHub repository.[65]

## Order parameters from experiments

The order parameter of a hydrocarbon C–H vector is defined as

$$S_{\mathrm{CH}} = \frac{1}{2}\langle 3\cos^2\theta - 1\rangle, \tag{1}$$

where the angle brackets denote an ensemble average over the sampled conformations, and $\theta$ is the angle between the C–H bond and the membrane normal. The absolute values of order parameters can be measured by detecting quadrupolar splitting with $^2$H NMR[66] or by detecting dipolar splitting with $^1$H-$^{13}$C NMR.[35,67–69] The measurements are based on different physical interactions, and also the connections between order parameter and quadrupolar or dipolar splitting are different. The absolute values of order parameters from the measured quadrupolar splitting $\Delta\nu_Q$ ($^2$H NMR) are calculated using the equation $|S_{\rm CD}| = \frac{4}{3}\frac{h}{e^2qQ}\Delta\nu_Q$, where the value for the static quadrupole splitting constant is estimated from various experiments to be 170 kHz leading to a numerical relation $|S_{\rm CD}| = 0.00784 \times \Delta\nu_Q$.[66] The absolute values of order parameters from the effective dipolar coupling $d_{\rm CH}$ ($^1$H-$^{13}$C NMR) are calculated using the equation $|S_{\rm CH}| = \frac{4\pi\langle r_{\rm CH}^3\rangle}{\hbar\mu_0\gamma_h\gamma_c}d_{\rm CH}$, where values between 20.2–22.7 kHz are used for $\frac{4\pi\langle r_{\rm CH}^3\rangle}{\hbar\mu_0\gamma_h\gamma_c}$, depending on the original authors.[35,67–69] The effective dipolar coupling $d_{\rm CH}$ is related to the measured dipolar splitting $\Delta\nu_{\rm CH}$ through a scaling factor that depends on the pulse sequence used in the $^1$H-$^{13}$C NMR experiment.[35,67–69] It is important to note that the order parameters measured with different techniques based on different physical interactions are in good agreement with each other (see Results and Discussion), indicating very high quantitative accuracy of the measurements. For a more detailed discussion, see Ref. 70.

The absolute values of order parameters are accessible with both $^2$H NMR and $^1$H-$^{13}$C NMR techniques. However, only $^1$H-$^{13}$C NMR techniques allow also the measurement of the sign of the order parameter.[16,67,68] The measured sign is negative for almost all the carbons discussed in this work, except for $\alpha$ which is positive.[16,67,68] For more detailed discussion about the determination of the sign of the order parameters, see Ref. 71.

For most $CH_2$ segments in a fluid phospholipid bilayer, the order parameters of both hydrogens are equal. However, in some cases (e.g., $g_1$, $g_3$, and $C_2$ carbon in the *sn*-2 chain) the two order parameters are not equal; this can be observed with both $^2$H NMR and $^1$H-$^{13}$C NMR techniques. In the present work, to avoid confusion with the dipolar and quadrupolar splittings in NMR terminology, we call the phenomenon of unequal order parameters for hydrogens attached to the same carbon *forking*. Forking has been studied in detail with $^2$H NMR techniques by deuterating the R or S position in $CH_2$ segment, and the studies show that it arises from differently sampled orientations of the two C–H bonds, not from two separate populations of lipid conformations.[26,72]

## Order parameters from simulations

The order parameters from simulations were calculated directly using the definition of Eq. 1. For the united atom models, the hydrogen positions were generated post-simulationally from the positions of the heavy atoms and the known hydrocarbon geometries. The statistical error was estimated based on the assumption that different lipids are statistically independent entities (which should be the case in fluid phase): The time average of a given order parameter was first calculated separately for each lipid, and the standard error of the mean over these time averages then taken as the error bar for this order parameter.

It has been pointed out that the sampling of individual dihedral angles might be very slow compared to the typical (100 ns) simulation timescales.[73] After 200 ns, however, even the slowest rotational correlation function of a C–H bond ($g_1$) reaches a plateau ($S^2_{\mathrm{CH}}$) in the Berger-POPC-07 model[74]—and, notably, the dynamics of this segment have been shown to be significantly slower in simulations than in experiments.[75] In practise, due to averaging over different lipid molecules, less than 200 ns of simulation data should be enough for the order parameter calculation; if the sampling within typical simulation times is not enough for the convergence of the order parameters, then the simulation model in question has unphysically slow dynamics.

## Simulated systems

All simulations are ran with a standard setup for a planar lipid bilayer in zero tension and constant temperature with periodic boundary conditions in all directions by using the

GROMACS software package[76] (version numbers 4.5.X–4.6.X), LAMMPS,[77] MDynaMix[78] or NAMD.[79] The number of molecules, simulation temperatures and the length of simulations of all the simulated systems are listed in Tables 1, 2 and 3. Full simulation details are given in the Supporting Information (SI) or in the original publications in case the data is used previously therein. All simulation parameters were set as close to the original parametrization works as possible. Additionally, the files related to the simulations and the resulting trajectories are publicly available for almost all systems in the Zenodo collection `https://zenodo.org/collection/user-nmrlipids`. The references pointing to simulation details and files are also listed in Tables 1, 2 and 3.

# Results and Discussion

## Full hydration: Experimental order parameters for the glycerol backbone and headgroup

The specific deuteration of $\alpha$-, $\beta$- and $g_3$- segments of DPPC has been successful, allowing the absolute values of the order parameters for these segments to be measured by $^2$H NMR.[48–50,54] In addition, the absolute values of order parameters for all glycerol backbone and choline headgroup segments in egg yolk lecithin,[67] DMPC,[16,68,69] DOPC,[141] and POPC[35,141] have been measured with several different implementations of $^1$H-$^{13}$C NMR experiments. Furthermore, for some systems the signs of the order parameters have been measured with $^1$H-$^{13}$C NMR techniques.[16,67,68] The experimental values of the glycerol backbone and choline order parameters from various publications,[35,50,54,68,69] with the signs measured in Refs. 16,67,68, are shown in Fig. 2.

In general there is a good agreement between the order parameters measured with different experimental NMR techniques: Almost all the reported values are within a variation of $\pm 0.02$ (which is also the error estimate given by Gross et al.[68]) for all fully hydrated PC bilayers, regardless of variation in their acyl chain composition and temperature. Exceptions

**Table 1: Fully hydrated single component lipid bilayer systems simulated for Fig. 2: 1,2-dimyristoyl-sn-glycero-3-phosphocholine (DMPC), dilauroylphosphatidylcholine (DLPC), dipalmitoylphosphatidylcholine (DPPC), and 1-palmitoyl-2-oleoylphosphatidylcholine (POPC). The bolded systems were used also for Fig. 3. $^a$ Number of lipid molecules. $^b$ Number of water molecules. $^c$ Temperature. $^d$ Total simulation time. $^e$ Time used for analysis. $^f$ Reference link for the downloadable simulation files; the data sets marked with $^*$ also include a part of the trajectory. $^g$ Reference for the full simulation details; the original publication is cited if simulation data from previously published work has been directly used, for other systems the simulation details are given in the Supporting Information. $^h$ Magnitudes from Fig. S4 of Klauda et al.,[31] signs matched to our simulations. $^i$ Magnitudes from Fig. 9 of Dickson et al.,[33] signs matched to our simulations.**

| Force field | lipid | $^a$N$_l$ | $^b$N$_w$ | $^c$T (K) | $^d$t$_{sim}$(ns) | $^e$t$_{anal}$ (ns) | $^f$Files | $^g$Details |
|---|---|---|---|---|---|---|---|---|
| Berger-DMPC-04[80] | DMPC | 128 | 5097 | 323 | 130 | 100 | [ 81]* | [ 82] |
| Berger-DPPC-98[83] | DPPC | 72 | 2864 | 323 | 60 | 30 | [ 84]* | SI |
| **Berger-POPC-07**[74] | POPC | 128 | 7290 | 298 | 270 | 240 | [ 85]* | [ 75] |
| CHARMM36[31] | DPPC | 72 | 2189 | 323 | 30 | 25 | [ 86]* | SI |
| CHARMM36[31] | DPPC | 72 | 2189 | 323 | 130 | - | - | [ 31]$^h$ |
| CHARMM36[31] | POPC | 72 | 2242 | 303 | 30 | 20 | [ 87]* | SI |
| **CHARMM36**[31] | POPC | 128 | 5120 | 303 | 200 | 100 | [ 88]* | SI |
| MacRog[89] | POPC | 288 | 12600 | 310 | 100 | 80 | [ 90]* | SI |
| **MacRog**[89] | POPC | 128 | 6400 | 310 | 400 | 200 | [ 91]* | SI |
| MacRog[89] | POPC | 288 | 14400 | 310 | 90 | 40 | [ 92]* | SI |
| GAFFlipid[33] | DPPC | 72 | 2197 | 323 | 90 | 50 | [ 93]* | SI |
| GAFFlipid[33] | DPPC | 72 | 2167 | 323 | 250 | 250 | - | [ 33]$^i$ |
| **GAFFlipid**[33] | POPC | 126 | 3948 | 303 | 137 | 32 | [ 94]* | SI |
| Lipid14[95] | POPC | 72 | 2234 | 303 | 100 | 50 | [ 96]* | SI |
| Poger[97] | DPPC | 128 | 5841 | 323 | 2×100 | 2×50 | [ 98,99]* | SI |
| Slipids[100] | DPPC | 128 | 3840 | 323 | 150 | 100 | [ 101]* | SI |
| Slipids[102] | POPC | 128 | 5120 | 303 | 200 | 150 | [ 103]* | SI |
| Kukol[104] | POPC | 512 | 20564 | 298 | 50 | 30 | [ 105]* | SI |
| Chiu[106] | POPC | 128 | 3552 | 298 | 56 | 50 | [ 107]* | SI |
| Högberg08[29] | DMPC | 98 | 3840 | 303 | 75 | 50 | [ 108]* | [ 29] |
| Högberg08[109] | POPC | 128 | 3840 | 303 | 100 | 80 | [ 110]* | [ 109] |
| Ulmschneiders[111] | POPC | 128 | 3328 | 310 | 100 | 50 | [ 112]* | SI |
| Tjörnhammar14[113] | DPPC | 144 | 7056 | 323 | 200 | 100 | [ 114]* | [ 113] |
| Botan-CHARMM36-UA[115] | DLPC | 128 | 3840 | 323 | 30 | 20 | [ 116] | SI |
| Lee-CHARMM36-UA[117] | DPPC | 72 | 2189 | 323 | 70 | 50 | [ 118]* | SI |

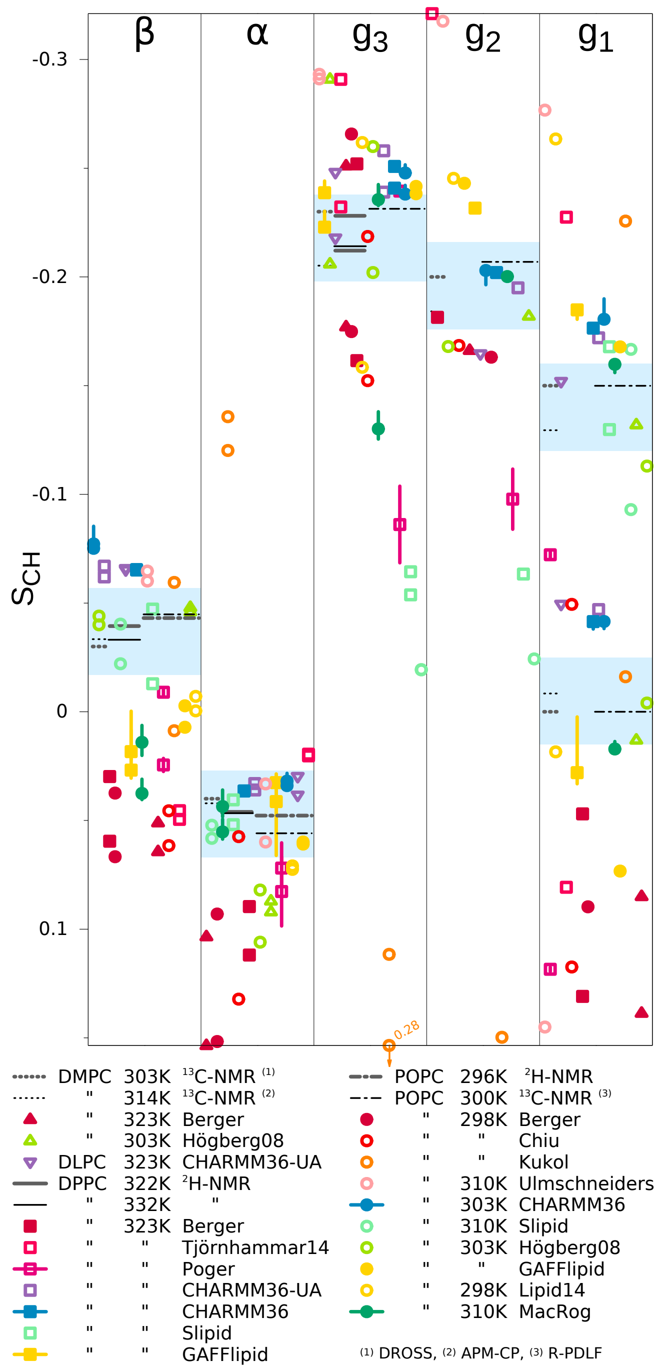


Figure 2: Order parameteres from simulations listed in Table 1 and experiments for glycerol and choline groups. The experimental values were taken from the following publications: DMPC 303 K from,[68] DMPC 314 K from,[69] DPPC 322 K from,[54] DPPC 323 K from,[50] POPC 296 K from,[45] and POPC 300 K from.[35] The vertical bars shown for some of the computational values are not error bars, but demonstrate that for these systems we had at least two data sets (see Table 1); the ends of the bars mark the extreme values from the sets, and the dot marks their measurement-time-weighted average. An interactive version of this figure is available at https://plot.ly/~HubertSantuz/72/lipid-force-field-comparison/.

**Table 2: Simulated single component lipid bilayers with varying hydration levels. The simulation file data sets marked with * include also part of the trajectory. $^a$ Water/lipid molar ratio $^b$ The number of lipid molecules $^c$ The number of water molecules $^d$ Simulation temperature $^e$ The total simulation time $^f$ Time frames used in the analysis $^g$ Reference link for the downloadable simulation files $^h$ Reference for the full simulation details**

| Force field | lipid | $^a$n (w/l) | $^b$N$_l$ | $^c$N$_w$ | $^d$T (K) | $^e$t$_{sim}$(ns) | $^f$t$_{anal}$ (ns) | $^g$Files | $^h$Details |
|---|---|---|---|---|---|---|---|---|---|
| Berger-POPC-07[74] | POPC | 57 | 128 | 7290 | 298 | 270 | 240 | [ 85]* | SI |
| | POPC | 7 | 128 | 896 | 298 | 60 | 50 | [ 119]* | SI |
| Berger-DLPC-13[120] | DLPC | 28 | 72 | 2016 | 300 | 80 | 60 | [ 121]* | [ 120] |
| | DLPC | 24 | 72 | 1728 | 300 | 80 | 60 | [ 122]* | [ 120] |
| | DLPC | 20 | 72 | 1440 | 300 | 80 | 60 | [ 123]* | [ 120] |
| | DLPC | 16 | 72 | 1152 | 300 | 80 | 60 | [ 124]* | [ 120] |
| | DLPC | 12 | 72 | 864 | 300 | 80 | 60 | [ 125]* | [ 120] |
| | DLPC | 8 | 72 | 576 | 300 | 80 | 60 | [ 126]* | [ 120] |
| | DLPC | 4 | 72 | 288 | 300 | 80 | 60 | [ 127]* | [ 120] |
| CHARMM36[31] | POPC | 40 | 128 | 5120 | 303 | 150 | 100 | [ 88]* | SI |
| | POPC | 31 | 72 | 2242 | 303 | 30 | 20 | [ 87]* | SI |
| | POPC | 15 | 72 | 1080 | 303 | 59 | 40 | [ 128]* | SI |
| | POPC | 7 | 72 | 504 | 303 | 60 | 20 | [ 129]* | SI |
| MacRog[89] | POPC | 50 | 288 | 14400 | 310 | 90 | 40 | [ 92]* | SI |
| | POPC | 44 | 288 | 12600 | 310 | 100 | 80 | [ 90]* | SI |
| | POPC | 25 | 288 | 7200 | 310 | 100 | 50 | [ 92]* | SI |
| | POPC | 20 | 288 | 5760 | 310 | 100 | 50 | [ 92]* | SI |
| | POPC | 15 | 288 | 4320 | 310 | 100 | 50 | [ 92]* | SI |
| | POPC | 10 | 288 | 2880 | 310 | 100 | 50 | [ 92]* | SI |
| | POPC | 5 | 288 | 1440 | 310 | 100 | 50 | [ 92]* | SI |
| GAFFlipid[33] | POPC | 31 | 126 | 3948 | 303 | 137 | 32 | [ 94]* | SI |
| | POPC | 7 | 126 | 896 | 303 | 130 | 40 | [ 130]* | SI |

are the somewhat lower order parameters reported from some measurements using $^1$H-$^{13}$C NMR.[16,67,141] In these experiments, however, the reported error bars are either relatively large,[16,67] or the spectral resolution is quite low and numerical lineshape simulations have not been used in the analysis.[141] As it, therefore, is highly likely that the reported lower order parameters are due to lower experimental accuracy, we exclude them from the present discussion; for more details, see Ref. 70. Motivated by the high experimental reproducibility, we have highlighted in Fig. 2 subjective sweet spots (light blue areas spanning 0.04 units around the average of the extremal experimental values), within which we expect the

**Table 3: Simulated lipid bilayers containing cholesterol. The simulation file data sets marked with * include also part of the trajectory. $^a$ The number of lipid molecules $^b$ The number of cholesterol molecules $^c$ Cholesterol concentration (mol%) $^d$ The number of water molecules $^e$ Simulation temperature $^f$ The total simulation time $^g$ Time frames used in the analysis $^h$ Reference link for the downloadable simulation files $^i$ Reference for the full simulation details**

| Force field | lipid | $^a N_l$ | $^b N_{chol}$ | $^c C_{CHOL}$ | $^d N_w$ | $^e$T (K) | $^f t_{sim}$(ns) | $^g t_{anal}$ (ns) | $^h$Files | $^i$Details |
|---|---|---|---|---|---|---|---|---|---|---|
| Berger-POPC-07[74] /Höltje-CHOL-13[35,131] | POPC | 128 | 0 | 0% | 7290 | 298 | 270 | 240 | [ 85]* | [ 75] |
| | POPC | 120 | 8 | 6% | 7290 | 298 | 100 | 80 | [ 132]* | [ 35] |
| | POPC | 110 | 18 | 14% | 8481 | 298 | 100 | 80 | [ 133]* | [ 35] |
| | POPC | 84 | 44 | 34% | 6794 | 298 | 100 | 80 | [ 134]* | [ 35] |
| | POPC | 64 | 64 | 50% | 10314 | 298 | 100 | 80 | [ 135]* | [ 35] |
| | POPC | 50 | 78 | 61% | 5782 | 298 | 100 | 80 | [ 136]* | [ 35] |
| CHARMM36[31,137] | POPC | 128 | 0 | 0% | 5120 | 303 | 150 | 100 | [ 88]* | SI |
| | POPC | 512 | 0 | 0% | 23943 | 298 | 170 | 100 | [ 138]* | SI |
| | POPC | 460 | 52 | 10% | 23569 | 298 | 170 | 100 | [ 138]* | SI |
| | POPC | 436 | 76 | 15% | 23331 | 298 | 170 | 100 | [ 138]* | SI |
| | POPC | 100 | 24 | 19% | 4960 | 303 | 200 | 100 | [ 139]* | SI |
| | POPC | 410 | 102 | 20% | 20972 | 298 | 170 | 100 | [ 138]* | SI |
| | POPC | 384 | 128 | 25% | 22327 | 298 | 170 | 100 | [ 138]* | SI |
| | POPC | 332 | 180 | 35% | 21340 | 298 | 170 | 100 | [ 138]* | SI |
| | POPC | 256 | 256 | 50% | 20334 | 298 | 170 | 100 | [ 138]* | SI |
| | POPC | 80 | 80 | 50% | 4496 | 303 | 200 | 100 | [ 140]* | SI |
| MacRog[89] | POPC | 128 | 0 | 0% | 6400 | 310 | 400 | 200 | [ 91]* | SI |
| | POPC | 114 | 14 | 11% | 6400 | 310 | 400 | 200 | [ 91]* | SI |
| | POPC | 72 | 56 | 44% | 6400 | 310 | 400 | 200 | [ 91]* | SI |
| | POPC | 64 | 64 | 50% | 6400 | 310 | 400 | 200 | [ 91]* | SI |
| | POPC | 56 | 72 | 56% | 6400 | 310 | 400 | 200 | [ 91]* | SI |

calculated values of the order parameters of a well-performing force field to fall.

In addition to the numerical values, forking (see Sec. ) is an important feature of the order parameters. In contrast to the lack of forking in the choline segments $\alpha$ and $\beta$, both $CH_2$ segments of the glycerol backbone fork. In the $g_3$ segment forking is small ($\approx 0.02$), and some experiments only report the larger or the average value.[35,50] However, forking is significant for the $g_1$ segment, whose lower order parameter is close to zero and the larger one has an absolute value of approximately 0.13–0.15. Forking was studied in detail by Gally et al.,[26] who used E. Coli to stereospecifically deuterate the different hydrogens attached to the $g_1$ or $g_3$ groups in PE lipids, and measured the order parameters from the lipid extract. This experiment gave the lower order parameter when deuterium was in the S position of $g_1$ or R position for $g_3$. Since the glycerol backbone order parameters are very similar irrespective of the headgroup chemistry (PC, PE, or PG) or lipid environment,[26] it is reasonable to assume that the stereospecifity measured for the PE lipids holds also for the PC lipids.

The most detailed experimentally available order parameter information for the glycerol backbone and choline segments of POPC bilayer is collected by taking the absolute values from Ref. 35, the signs from Refs. 16,67,68 and the stereospecific labeling from Ref. 26, and is shown in Fig. 3.

## Full hydration: Comparison between simulation models and experiments

The order parameters of the glycerol backbone and headgroup calculated from different force fields for various lipids have been previously compared to experiments.[28–37] The general conclusion from these studies seems to be that the CHARMM based,[29,31] GAFFlipid[33] and MacRog[37] force fields perform better for the glycerol backbone and headgroup structures than the GROMOS based models.[30,32,34,35] However, none of the studies exploits the full potential of the available experimental data discussed in the previous section, i.e. the quantitative accuracy, known signs and stereospecific labeling of the experimental order

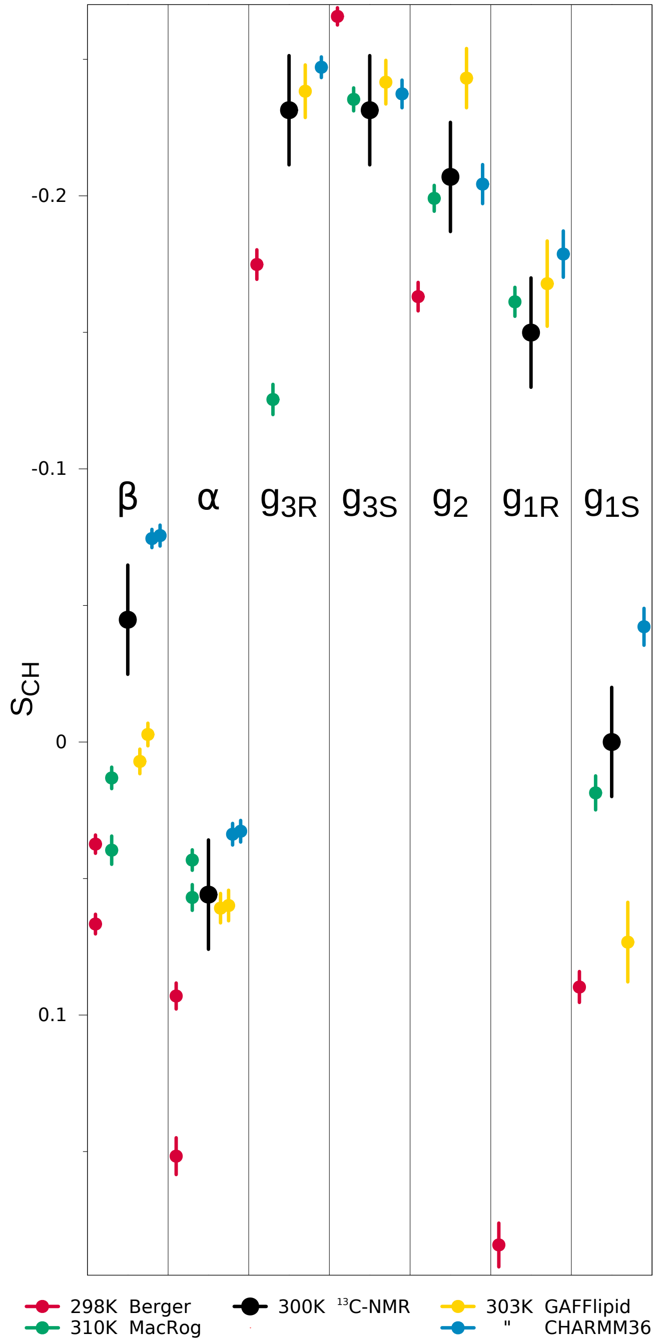


Figure 3: Order parameteres for POPC glycerol and choline groups from simulations with Berger-POPC-07, MacRog, GAFFlipid, and CHARMM36 force fields (the **bolded** systems in Table 1) together with experimental values. The error bars of simulation data are standard errors of mean (see Methods for details). The magnitudes for experimental order parameters are taken from Ferreira et al.,[35] the signs are based on the measurements by Hong et al.[16,67] and Gross et al.,[68] and the R/S labeling is based on the measurements by Gally et al.[26]

parameters.

To get a general idea of the quality of the glycerol backbone and choline headgroup structures in different models, we calculated the order parameters for these parts from thirteen different lipid models (Table 1) and plotted the results together with experimental values in Fig. 2. Two criteria were used to judge the quality of the model: 1) there must not be significant **forking** in the $\alpha$ and $\beta$ carbons, there must be only moderate forking in the $g_3$ carbon and there must be significant forking in the $g_1$ carbon, and 2) the **magnitude** should be preferably inside to the subjective sweet spots determined from experiments (blue shaded regions in Fig. 2). The results for each force field with respect to the above criteria are summarized in Figure 4.

None of the studied force fields fulfils these criteria completely, however CHARMM36 is close. This is not surprising since the dihedral potentials in this model are tuned against experiments to better reproduce these order parameters.[31] The next models in the list are CHARMM36-UA[115,117] and Högberg08,[29] which is also not surprising since these models are using the CHARMM bonded potentials for glycerol backbone and choline. The fourth and the fifth models in the list, MacRog[37] and GAFFlipid,[33] have independently determined dihedral potentials. All the models based on Gromos potentials and Slipids perform less well. In the following sections we subject CHARMM36, MacRog, GAFFlipid and Berger-POPC-07 to a more careful comparison including the stereospecific labeling (Fig. 3), atomistic level structure, and responses to dehydration and cholesterol content. These models are selected for more detailed study since they are the best representatives of different dihedral potential parametrization techniques (CHARMM36, MacRog, GAFFlipid), and the Berger based models are the most used lipid models in the literature.

## Full hydration: Atomistic resolution structures in different models

The results in the previous section revealed significant differences of the glycerol backbone and choline headgroup order parameters between different molecular dynamics simulation

| | $\beta$ | $\alpha$ | $g_3$ | $g_2$ | $g_1$ | $\Sigma$ |
|---|---|---|---|---|---|---|
| CHARMM 36 | M | | M | | M | 3 |
| CHARMM 36-UA | M | F | M | M | M F | 6 |
| Hög-berg08 | | M F | M F | M | F | 8 |
| MacRog | M F | F | M F | | M F | 8 |
| GAFFlipid | M F | F | M F | M | M F | 9 |
| Lipid14 | M F | M | M F | M | M F | 11 |
| Chiu | M F | M F | M F | M | M F | 11 |
| Ulm-schneiders | M | F | M F | M | M F | 12 |
| Slipid | F | F | M F | M | M F | 13 |
| Poger | M F | M F | M F | M | M F | 13 |
| Tjörn-hammar14 | M | M | M F | M | M F | 15 |
| Berger | M F | M F | M F | M | M F | 15 |
| Kukol | M F | M F | M F | M | M F | 16 |

Figure 4: Rough subjective ranking of force fields based on Fig. 2. Here "M" indicates a magnitude problem, "F" a forking problem; letter size increases with problem severity. Color scheme: "within experimental error" (dark green), "almost within experimental error" (light green), "clear deviation from experiments" (light red), and "major deviation from experiments" (dark red). The $\Sigma$-column shows the total deviation of the force field, when individual carbons are given weights of 0 (matches experiment), 1, 2, and 4 (major deviation). For full details of the assessment, see Supporting Information.

models. However, it is not straightforward to conclude which kind of structural differences (if any) between the models the results indicate, because the mapping from the order parameters to the structure is not unique. In this section we demonstrate that 1) the differences in order parameters indicate significantly different structural sampling, which is strongly correlated with the dihedral angles of the related bonds; and that 2) the comparison between experimental and simulated order parameters can be used to exclude nonrealistic structural sampling in molecular dynamics simulations. The demonstration is done for the dihedral angles defined by the $g_3$-$g_2$-$g_1$-O(*sn*-1) segments in the glycerol backbone and the N-$\beta$-$\alpha$-O segments in the headgroup. These dihedrals were chosen for demonstration, because significant differences between the models are observed around these segments in Fig. 3. We note that performing a similar comparison through all the dihedrals in all the 13 models would probably give highly useful information on how to improve the accuracy of the models; yet this is beyond the scope of the current report.

The dihedral angle distributions for the $g_3$-$g_2$-$g_1$-O(*sn*-1) dihedral calculated from different models are shown in Fig. 5. The distribution is qualitatively different for the Berger-POPC-07 model, showing a maximum in the gauche$^+$-conformation ($60^o$) compared to all the other models showing a maximum in the anti-conformation ($180^o$). The distributions in all the other models have the same general features, the main difference being that the fraction of configurations in the gauche$^-$-conformation ($-60^o$) is zero for the MacRog, detectable for the CHARMM36 and equally large to the gauche$^+$ fraction in GAFFlipid. From the results we conclude that most likely the wrongly sampled dihedral angle for the $g_2$-$g_1$ bond explains the significant discrepancy to the experimental order parameters for the $g_1$ segment in the Berger-POPC-07 model (Fig. 3). In conclusion, models preferring the anti conformation for this dihedral give more realistic order parameters; this is in agreement with previous crystal structure and $^1$H NMR studies.[19–21,23–25]

The dihedral angle distribution for the N-$\beta$-$\alpha$-O dihedral calculated from the same four models is shown in Fig. 6. Also for this dihedral there are significant differences in the

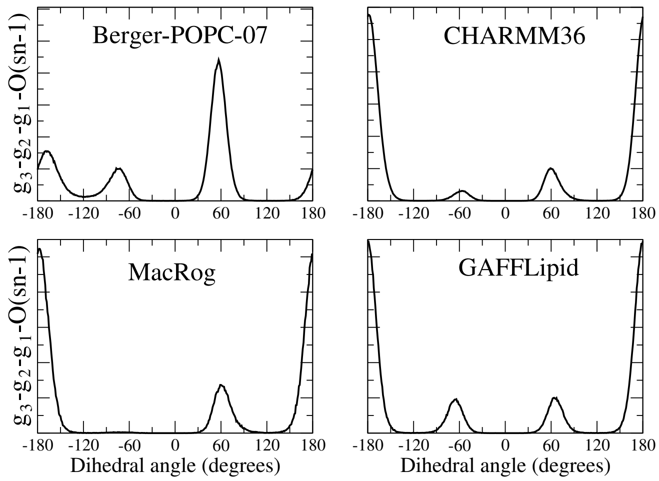


Figure 5: Dihedral angle distributions for $g_3$-$g_2$-$g_1$-O($sn$-1) dihedral from different models (POPC bilayer in full hydration).

gauche–anti fractions. The gauche conformations are dominant in CHARMM36, in MacRog there are only anti conformations present, and in Berger-POPC-07 and GAFFlipid the gauche and anti conformations have equal probabilities. On the other hand, comparison of $\alpha$ and $\beta$ order parameters in Fig. 3 reveals that for these carbons the CHARMM36 is closest to the experimental results and it is also the only model that has the correct sign (negative) for the $\beta$ order parameter. This result is again in agreement with previous crystal structure, $^1$H NMR, and Raman spectroscopy studies,[19–22] which suggest that this dihedral is in the gauche conformation in the absence of ions.

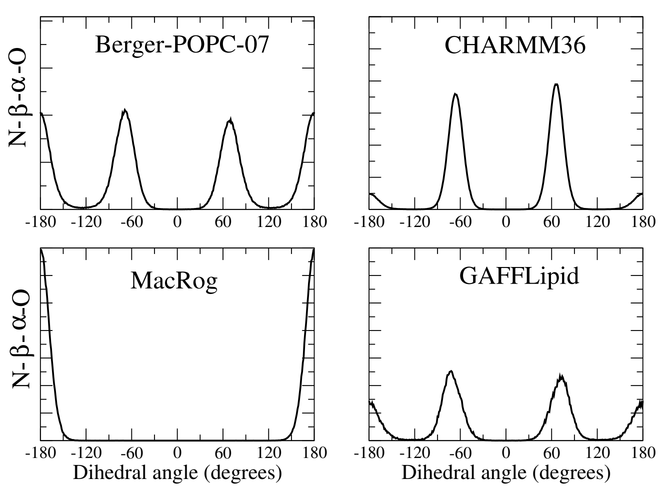


Figure 6: Dihedral angle distributions for N-$\beta$-$\alpha$-O dihedral from different models (POPC bilayer in full hydration).

These examples show that the glycerol backbone and headgroup order parameters reflect the atomistic resolution structure and that the comparison with experiments allows the assessment of the quality of the suggested structure. We were able to pinpoint specific problems in the structures in different models and suggest potential improvement strategies. If an improved atomistic molecular dynamics simulation model would reproduce the order parameters and other experimental observables (like $^{31}$P chemical shift anisotropy[36] and $^{31}$P-$^{13}$C dipolar couplings[43]) within experimental accuracy, it would give an interpretation for the atomistic resolution structure of the glycerol backbone and choline.[10–13,15,16,18] The research along these lines is left, however, for future studies.

## Response to dehydration and cholesterol content

In addition to pure phosphatidylcholine bilayers at full hydration, the choline headgroup order parameters have been measured under various different conditions.[30,32,35,45–51,54,55] Also the order parameters for the glycerol backbone have been measured with $^{1}$H-$^{13}$C NMR in dehydrated conditions,[47] and as a function of anesthetics[30] and glycolipids[32] for DMPC, and as a function of cholesterol concentration for POPC.[35] Due to the high resolution in the NMR (especially $^{2}$H NMR) experiments, even very small order parameter changes resulting from the varying conditions can be measured (see Ref. 70 for more discussion)—but, as already discussed above, it is not simple to deduce the structural changes from order parameter changes.[15,18] However, comparison of the order parameters between simulations and experiments in different conditions can be used to assess the quality of the force field in different situations, and, if the quality is good, to interpret the structural changes in experiments. Here we exemplify such comparison for a lipid bilayer under low hydration levels and when varying amounts of cholesterol is included in the bilayer. The interaction between ions and a phosphatidylcholine bilayer will be discussed in a separate study.[60]

## Phospholipid bilayer with low hydration level

Fig. 7 shows the published[45–47] experimental order parameters for the glycerol backbone and choline as a function of hydration level. Despite slight differences in temperature and acyl chain composition, the three independently reported data sets for the choline ($\beta$ and $\alpha$) segments agree well with each other: Both order parameters increase with decreasing hydration level. The glycerol backbone order parameters ($g_3$, $g_2$, $g_1$), in contrast, have been observed[47] to slightly decrease with dehydration. Note that the original experiments[45–47] measured only absolute values, but here we included the signs measured in separate studies.[16,67,68] Consequently, the negative $\beta$ order parameter actually increases with dehydration as its absolute value decreases.[45–47]

Lipid bilayer dehydration has been studied also with molecular dynamics simulations,[142–147] typically motivated by the discussion concerning the origin of the "hydration repulsion".[148–150] Only one[142] of these studies, however, compared their simulation model to the experimental choline and glycerol backbone order parameters. Fig. 7 shows these order parameters as a function of hydration level for the CHARMM36, MacRog and GAFFlipid models (having the most realistic atomistic resolution structures) and a Berger-based model (which is the most used lipid model); note that the simulation results have been vertically shifted to ease the comparison with experimental response to dehydration. Despite of some fluctuations, the increase of the choline ($\beta$ and $\alpha$) order parameters is seen in all four models. The response of the choline order parameters to dehydration can, therefore, be interpreted to qualitatively agree with experiments. The situation is significantly more complicated for the glycerol backbone: None of the four models produced the experimentally seen trends in all the ($g_3$, $g_2$, $g_1$) segments.

The qualitative agreement of the $\alpha$ and $\beta$ order parameters with experiments in all four simulation models (Fig. 7) indicates that, despite the unrealistic structures at full hydration (Figs. 2 and 4), the structural response of the choline headgroup to dehydration is somewhat realistic. A likely explanation is that as the interlamellar space shrinks with dehydration,

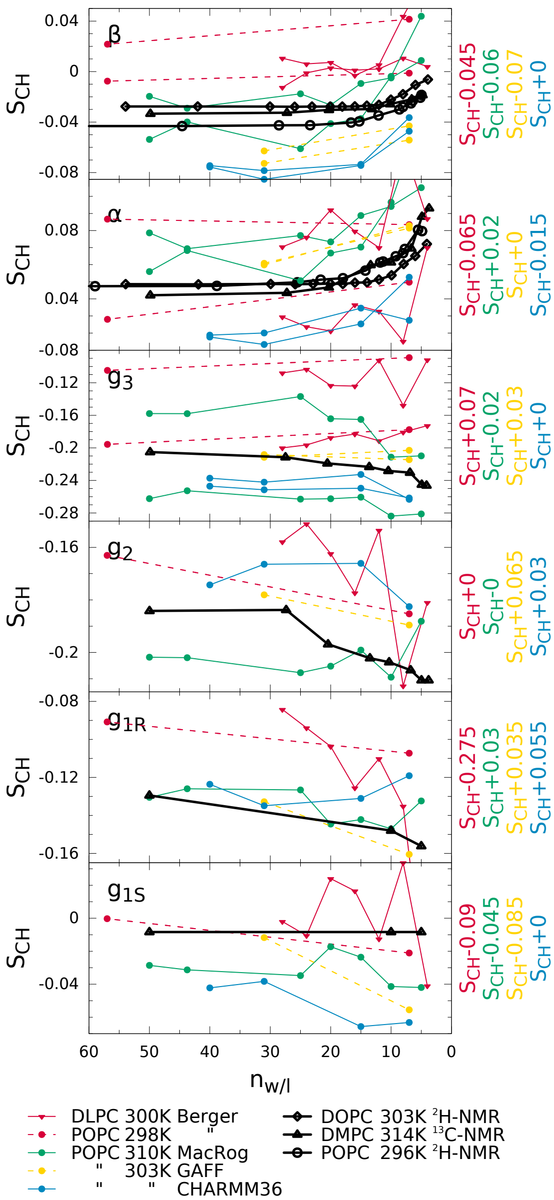


Figure 7: The effect of dehydration on glycerol and choline order parameters in experiments. The magnitudes of order parameters are measured for DMPC ($^1$H-$^{13}$C NMR) at 314 K,[47] for POPC ($^2$H NMR) at 296 K[45] and for DOPC ($^2$H NMR) at 303 K.[46] The signs are based on the measurements by Hong et al.[16,67] and Gross et al.[68] Note that to elucidate the relative change as a function of hydration level, the simulation results were vertically shifted; the shift magnitudes for each of the force fields are listed ($S_{CH}$+shift) in the y-label.

the whole choline group orients more parallel to the membrane. Indeed, upon dehydration the angle between P–N (phoshate phosphorus to choline nitrogen) vector and membrane normal increases for all the four models (Fig. 8). However, the amount of increase depends on the model. Especially the DLPC simulations with Berger model predict significantly stronger P–N vector tilt than the other models. The Berger model has also generally larger P–N vector angles and its choline order parameters are more off from experiments than the other three models (Fig. 3). Thus the relatively modest tilting with dehydration predicted by MacRog, CHARMM36 and GAFFlipid is probably more realistic.

It must be stressed that in the models incapable of reproducing the experimental order parameters the free energy landscape is not correct. Thus even though the order parameter response to dehydration is qualitatively correct, the energetic response is likely to be incorrect. This may have some influence on dehydration energetic calculations made using the Berger model.[145,147]

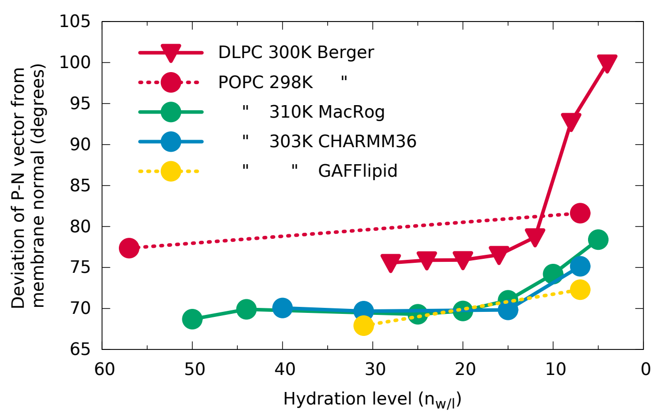


Figure 8: The average angle between membrane normal and P–N vector as function of hydration level calculated from different simulations.

The response of the glycerol backbone seems to be more subtle than that of the choline headgroup; none of the four models reproduced the experimental trends upon dehydration with enough accuracy to invite a structural interpretation.

### Cholesterol-containing phospholipid bilayer

As cholesterol is abundant in biological membranes and has been suggested to be an important player, for example, in domain formation,[151,152] phospholipid–cholesterol interactions have been extensively studied with theoretical[153–156] and experimental[8,35,48,157] methods. It is widely agreed that cholesterol orders lipid acyl tails and thus decreases the area per molecule (condensing effect), but its influence on the lipid headgroup and glycerol backbone remains debated.[151–153] It has been suggested, for example, that the surrounding phospholipids shield cholesterol from exposure to water by reorienting their headgroups ("umbrella model")[153] or that cholesterol acts as a spacer between the headgroups to increase their entropy and dynamics ("superlattice model").[152] Molecular dynamics simulations have supported both the umbrella[156] as well as the superlattice[154] model, in addition to suggesting specific interactions of cholesterol with the glycerol backbone.[155] In these studies[154–156] the responses of the glycerol backbone and choline headgroup to increasing cholesterol content were not, however, compared to experiments.

Fig. 9 shows the responses of the choline headgroup ($\beta$ and $\alpha$) order parameters of POPC (measured by $^1$H-$^{13}$C NMR[35]) and DPPC ($^2$H NMR[48]) to increasing cholesterol content. Again, the two independent data sets agree very well: Only very modest ($\Delta S_{\mathrm{CH}} < 0.03$) changes occur in the choline order parameters as cholesterol content increases from 0 to 60%. The extreme sensitivity of the high resolution $^2$H NMR experiments is beautifully demonstrated by the measurable[48] (but barely visible on the scale used in Fig. 9) cholesterol-induced forking of the $\alpha$ order parameter.

We note that the modest ($\Delta S_{\mathrm{CH}} < 0.02$ for $g_1$; $< 0.04$ for $g_2$, $g_3$; see Fig. 9) effects of cholesterol on the glycerol backbone order parameters of POPC measured by $^1$H-$^{13}$C NMR[35] agree well with the results for phosphatidylethanolamine (PE) measured by $^2$H NMR.[158] This further supports the ideas that the glycerol backbone structural behaviour is independent of the headgroup composition[26] and that the headgroup structure is largely independent of the acyl chain region content unless charges are present.[27]

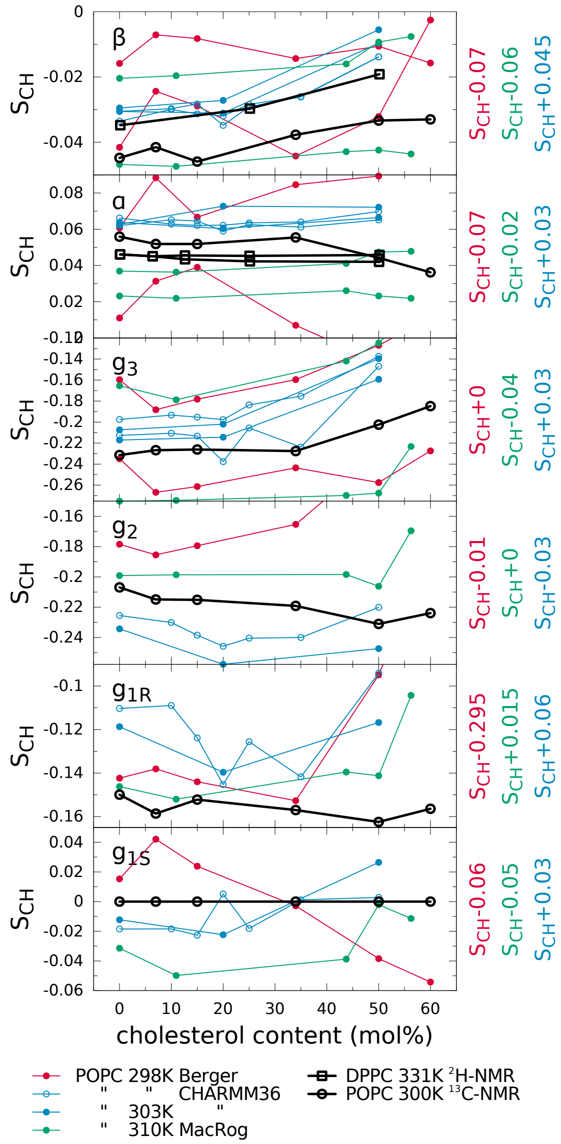


Figure 9: The effect of cholesterol content on the glycerol backbone and choline order parameters in experiments[35,48] and simulations with the Berger-POPC-07/Höltje-CHOL-13, CHARMM36 and MacRog force fields. The signs in the experimental values are based on the measurements by Hong et al.[16,67] and Gross et al.[68] In order to elucidate the relative change as a function of cholesterol content, the simulation results were vertically shifted; the shift magnitudes for each of the force fields are listed ($S_{CH}$+shift) in the y-label.

In addition to the experimental data, Fig. 9 shows our results for the CHARMM36 and MacRog force fields and the previously published[35] Berger-POPC-07/Höltje-CHOL-13 results. Note that the simulation data are shifted vertically to ease comparison with experimental responses. As previously pointed out,[35] the Berger-based model seriously exaggerates the effect of cholesterol on the phospholipid glycerol backbone and choline headgroup. In comparison, the choline and glycerol backbone responses of CHARMM36 and MacRog are in better qualitative agreement with experiments. Therefore, to resolve the nature of cholesterol-induced structural changes, we calculated from CHARMM36 the glycerol backbone orientation and dihedral angle distributions at various cholesterol contents (Supporting Information). The only detectable changes are the small decrease of gauche(-) and increase of gaughe(+) probability of the $g_3$-$g_2$-$g_1$-O(*sn*-1) dihedral and slight (less than 5 degrees) change in the glycerol backbone orientation. In conclusion, our results suggest that the significant effects of cholesterol on lipid conformations observed in simulations[154–156] are overestimated by the computational models used; cholesterol only induces very small structural changes in the glycerol backbone.

Finally, it is important to note that the CHARMM36 force field parameters (glycerol backbone dihedral potentials) have been tuned to reproduce the experimental order parameters at full hydration.[31] This approach introduces a risk of overfitting, which would manifest itself as wrong responses to changing conditions. Interestingly, according to our results, tuning did not lead to overfitting problems as far as dehydration or cholesterol content are considered.

# Conclusions

The atomistic resolution structures sampled by the glycerol backbone and choline headgroup in phoshatidylcholine bilayers are not known despite of vast amount of accurate experimental data. An atomistic resolution molecular dynamics simulation model that would reproduce the experimental data would automatically resolve the structures, thus giving an unprecedently detailed interpretation of the experimental data. In this work we have collected and reviewed the experimental C–H bond vector order parameters available in the literature. These accurate experimental data are then compared to 13 different atomistic resolution simulation models for a fully hydrated lipid bilayer system, followed by bilayers dehydrated to different extents, and finally bilayers containing various amounts of cholesterol. We are led to the following four main conclusions:

(1) The C–H bond order parameters measured with different NMR techniques are consistent. By combining the experimental results from various sources we concluded that the order parameters for each C–H bond are known with a quantitative accuracy of $\pm 0.02$.

(2) Comparison of order parameters between experiments and different atomistic resolution models together with structural analysis showed that the order parameters can be used to judge the structural accuracy of a model. Thus the combination of atomistic resolution molecular dynamics simulations and NMR experiments can be used to resolve the atomistic resolution structures of biomolecules in biologically relevant conditions. This approach can be extended from lipids to, for example, membrane proteins.

(3) The review of previous experimental results revealed that when a bilayer is dehydrated the choline order parameters increase. Our simulations suggested that this can be explained by the P–N vector tilting more parallel to the membrane. This strongly supports and complements the idea that charge-induced choline tilting can be measured using order parameter changes.[55,60]

(4) Only modest changes of glycerol backbone and choline order parameters are observed experimentally with increasing cholesterol content. When interpreted using the computa-

tional lipid model that we found to have the most realistic response to cholesterol, this observation means that cholesterol induces only minor changes in the $g_3$-$g_2$-$g_1$-O(sn-1) dihedral of the glycerol backbone, in other words, there is no major conformational change of the lipid.

(+) Besides these four main conclusions, we note that we have created the most extensive publicly available collection of molecular dynamics simulation trajectories of lipid bilayers (`https://zenodo.org/collection/user-nmrlipids`). The mere existence of this collection opens up numerous possibilities for unforeseen analyses, such as data mining, and rapid testing of ideas with much less computational effort than previously required.

In general, we conclude that in order to fully utilize the potential of atomistic-resolution classical molecular dynamics simulations in the structural interpretation of high resolution NMR data[159] for lipid bilayers, one must improve the phoshatidylcholine glycerol backbone and choline headgroup parameters of the existing force fields.

This work has been done as a fully open collaboration, using `nmrlipids.blogspot.fi` as the communication platform. All the scientific contributions have been communicated publicly through this blog.[61]

## Acknowledgement

We acknowledge all the discussion participants at `nmrlipids.blogspot.fi`. AB and CL acknowledge financial support from the French National Research Agency (ANR: Biolubrication by phospholipid membranes, Biolub2012) and computing time allocation from Pôle Scientifique de Modélisation Numérique from the ENS Lyon (PSMN), and Centre Informatique National de l'Enseignement Supérieur (CINES, Montpelier, France) (Project c2015096850). FFR acknowledges CONACYT and DGAPA UNAM IG100513 for financial support, Cluster Híbrido de Supercómputo Xiuhcoatl - CINVESTAV and Miztli - UNAM for computational resources. MJ and JT acknowledge and CSC – IT Center for Science for computational resources (project number tty3979). MJ also acknowledges the Finnish Doctoral Programme in

Computational Sciences (FICS) for funding. JT, MJ, TR and WK acknowledge the funding from the Academy of Finland (Centre of Excellence program) and the European Research Council (Advanced Grant project CROWDED-PRO-LIPIDS). WK acknowledges CSC – IT Centre for Science (Espoo, Finland) for excellent computational resources (project number tty3995). MSM acknowledges financial support from the Volkswagen Foundation (86110). LM acknowledges funding proved by the Institut national de la santé et de la recherche médicale (INSERM). JM acknowledges CSC – IT Center for Science for computational resources. OHSO acknowledges Tiago Ferreira and Paavo Kinnunen for useful discussions, the Emil Aaltonen foundation for financial support, Aalto Science – IT project and CSC – IT Center for Science for computational resources. HS acknowleges Catherine Etchebest and Stéphane Téletchéa for useful discussions and continued support, the HPC resources granted from GENCI-CINES (Grant 2014-c2014077209) and computer facilities provided by Région Ile de France and INTS (SESAME 2009 project).

## Supporting Information Available

Simulation and analysis details, two figures, and author contributions.

This material is available free of charge via the Internet at `http://pubs.acs.org/`.

## References

(1) Lipowsky, R., Sackmann, E., Eds. *Structure and Dynamics of Membranes*; Elsevier, 1995.

(2) Tieleman, D. P.; Marrink, S. J.; Berendsen, H. J. C. A computer perspective of membranes: molecular dynamics studies of lipid bilayer systems. *Biochim. Biophys. Acta* **1997**, *1331*, 235–270.

(3) Klauda, J. B.; Venable, R. M.; Jr., A. D. M.; Pastor, R. W. In *Computational Modeling*

*of Membrane Bilayers*; Feller, S. E., Ed.; Current Topics in Membranes; Academic Press, 2008; Vol. 60; pp 1 – 48.

(4) Edholm, O. In *Computational Modeling of Membrane Bilayers*; Feller, S. E., Ed.; Current Topics in Membranes; Academic Press, 2008; Vol. 60; pp 91 – 110.

(5) Tieleman, D. P. In *Molecular Simulations and Biomembranes: From Biophysics to Function*; Sansom, M., Biggin, P., Eds.; The Royal Society of Chemistry, 2010; pp 1–25.

(6) Piggot, T. J.; Piñeiro, Á.; Khalid, S. Molecular Dynamics Simulations of Phosphatidylcholine Membranes: A Comparative Force Field Study. *J. Chem. Theory Comput.* **2012**, *8*, 4593–4609.

(7) Rabinovich, A.; Lyubartsev, A. Computer simulation of lipid membranes: Methodology and achievements. *Polymer Science Series C* **2013**, *55*, 162–180.

(8) Marsh, D. *Handbook of Lipid Bilayers, Second Edition*; RSC press, 2013.

(9) Israelachvili, J. N.; Marcelja, S.; Horn, R. G. Physical Principles of Membrane Organization. *Q. Rev. Biophys.* **1980**, *13*, 121–200.

(10) Seelig, J.; Gally, H.-U.; Wohlgemuth, R. Orientation and flexibility of the choline head group in phosphatidylcholine bilayers. *Biochim. Biophys. Acta* **1977**, *467*, 109 – 119.

(11) Skarjune, R.; Oldfield, E. Physical studies of cell surface and cell membrane structure. Determination of phospholipid head group organization by deuterium and phosphorus nuclear magnetic resonance spectroscopy. *Biochemistry* **1979**, *18*, 5903–5909.

(12) Jacobs, R. E.; Oldfield, E. {NMR} of membranes. *Prog. Nucl. Mag. Res. Sp.* **1980**, *14*, 113 – 136.

(13) Davis, J. H. The description of membrane lipid conformation, order and dynamics by 2H-NMR. *Biochim. Biophys. Acta* **1983**, *737*, 117 – 171.

(14) Strenk, L.; Westerman, P.; Doane, J. A model of orientational ordering in phosphatidylcholine bilayers based on conformational analysis of the glycerol backbone region. *Biophys. J.* **1985**, *48*, 765 – 773.

(15) Akutsu, H.; Nagamori, T. Conformational analysis of the polar head group in phosphatidylcholine bilayers: a structural change induced by cations. *Biochemistry* **1991**, *30*, 4510–4516.

(16) Hong, M.; Schmidt-Rohr, K.; Nanz, D. Study of phospholipid structure by 1H, 13C, and 31P dipolar couplings from two-dimensional {NMR}. *Biophys. J.* **1995**, *69*, 1939 – 1950.

(17) Hong, M.; Schmidt-Rohr, K.; Zimmermann, H. Conformational Constraints on the Headgroup and sn-2 Chain of Bilayer DMPC from NMR Dipolar Couplings. *Biochemistry* **1996**, *35*, 8335–8341.

(18) Semchyschyn, D. J.; Macdonald, P. M. Conformational response of the phosphatidylcholine headgroup to bilayer surface charge: torsion angle constraints from dipolar and quadrupolar couplings in bicelles. *Magn. Res. Chem.* **2004**, *42*, 89–104.

(19) Hauser, H.; Guyer, W.; Pascher, I.; Skrabal, P.; Sundell, S. Polar group conformation of phosphatidylcholine. Effect of solvent and aggregation. *Biochemistry* **1980**, *19*, 366–373.

(20) Hauser, H.; Guyer, W.; Paltauf, F. Polar group conformation of 1,2-di-O-alkylglycerophosphocholines in the absence and presence of ions. *Chem. Phys. Lipids* **1981**, *29*, 103 – 120.

(21) Hauser, H.; Pascher, I.; Pearson, R.; Sundell, S. Preferred conformation and molecular packing of phosphatidylethanolamine and phosphatidylcholine. *Biochim. Biophys. Acta* **1981**, *650*, 21 – 51.

(22) Akutsu, H. Direct determination by Raman scattering of the conformation of the choline group in phospholipid bilayers. *Biochemistry* **1981**, *20*, 7359–7366.

(23) Pascher, I.; Lundmark, M.; Nyholm, P.-G.; Sundell, S. Crystal structures of membrane lipids. *Biochim. Biophys. Acta* **1992**, *1113*, 339 – 373.

(24) Hauser, H.; Pascher, I.; Sundell, S. Preferred conformation and dynamics of the glycerol backbone in phospholipids. An NMR and x-ray single-crystal analysis. *Biochemistry* **1988**, *27*, 9166–9174.

(25) Marsh, D.; Páli, T. Lipid conformation in crystalline bilayers and in crystals of transmembrane proteins. *Chem. Phys. Lipids* **2006**, *141*, 48 – 65.

(26) Gally, H. U.; Pluschke, G.; Overath, P.; Seelig, J. Structure of Escherichia coli membranes. Glycerol auxotrophs as a tool for the analysis of the phospholipid head-group region by deuterium magnetic resonance. *Biochemistry* **1981**, *20*, 1826–1831.

(27) Scherer, P.; Seelig, J. Structure and dynamics of the phosphatidylcholine and the phosphatidylethanolamine head group in L-M fibroblasts as studied by deuterium nuclear magnetic resonance. *The EMBO journal* **1987**, *6*.

(28) Shinoda, W.; Namiki, N.; Okazaki, S. Molecular dynamics study of a lipid bilayer: Convergence, structure, and long-time dynamics. *J. Chem. Phys.* **1997**, *106*, 5731–5743.

(29) Högberg, C.-J.; Nikitin, A. M.; Lyubartsev, A. P. Modification of the CHARMM force field for DMPC lipid bilayer. *J. Comput. Chem.* **2008**, *29*, 2359–2369.

(30) Castro, V.; Stevensson, B.; Dvinskikh, S. V.; Högberg, C.-J.; Lyubartsev, A. P.; Zimmermann, H.; Sandström, D.; Maliniak, A. {NMR} investigations of interactions between anesthetics and lipid bilayers. *Biochim. Biophys. Acta - Biomembranes* **2008**, *1778*, 2604 – 2611.

(31) Klauda, J. B.; Venable, R. M.; Freites, J. A.; O'Connor, J. W.; Tobias, D. J.; Mondragon-Ramirez, C.; Vorobyov, I.; Jr, A. D. M.; Pastor, R. W. Update of the CHARMM All-Atom Additive Force Field for Lipids: Validation on Six Lipid Types. *J. Phys. Chem. B* **2010**, *114*, 7830–7843.

(32) Kapla, J.; Stevensson, B.; Dahlberg, M.; Maliniak, A. Molecular Dynamics Simulations of Membranes Composed of Glycolipids and Phospholipids. *J. Phys. Chem. B* **2012**, *116*, 244–252.

(33) Dickson, C. J.; Rosso, L.; Betz, R. M.; Walker, R. C.; Gould, I. R. GAFFlipid: a General Amber Force Field for the accurate molecular dynamics simulation of phospholipid. *Soft Matter* **2012**, *8*, 9617–9627.

(34) Poger, D.; Mark, A. E. Lipid Bilayers: The Effect of Force Field on Ordering and Dynamics. *J. Chem. Theory Comput.* **2012**, *8*, 4807–4817.

(35) Ferreira, T. M.; Coreta-Gomes, F.; Ollila, O. H. S.; Moreno, M. J.; Vaz, W. L. C.; Topgaard, D. Cholesterol and POPC segmental order parameters in lipid membranes: solid state 1H-13C NMR and MD simulation studies. *Phys. Chem. Chem. Phys.* **2013**, *15*, 1976–1989.

(36) Chowdhary, J.; Harder, E.; Lopes, P. E. M.; Huang, L.; MacKerell, A. D.; Roux, B. A Polarizable Force Field of Dipalmitoylphosphatidylcholine Based on the Classical Drude Model for Molecular Dynamics Simulations of Lipids. *J. Phys. Chem. B* **2013**, *117*, 9142–9160.

(37) Maciejewski, A.; Pasenkiewicz-Gierula, M.; Cramariuc, O.; Vattulainen, I.; Rog, T. Refined OPLS All-Atom Force Field for Saturated Phosphatidylcholine Bilayers at Full Hydration. *J. Phys. Chem. B* **2014**, *118*, 4571–4581.

(38) Robinson, A.; Richards, W.; Thomas, P.; Hann, M. Head group and chain behavior in

biological membranes: a molecular dynamics computer simulation. *Biophys. J.* **1994**, *67*, 2345 – 2354.

(39) Essex, J. W.; Hann, M. M.; Richards, W. G. Molecular Dynamics Simulation of a Hydrated Phospholipid Bilayer. *Philos. T. Roy. Soc. B* **1994**, *344*, 239–260.

(40) Kothekar, V. Molecular dynamics simulation of hydrated phospholipid bilayers. *Ind. J. Biochem. Biophys.* **1996**, *33*, 431 – 447.

(41) Hyvönen, M. T.; Rantala, T. T.; Ala-Korpela, M. Structure and Dynamic Properties of Diunsaturated 1-Palmitoyl-2-Linoleoyl-sn-Glycero-3-Phosphatidylcholine Lipid Bilayer from Molecular Dynamics Simulation. *Biophys. J.* **1997**, *73*, 2907–2923.

(42) Duong, T. H.; Mehler, E. L.; Weinstein, H. Molecular Dynamics Simulation of Membranes and a Transmembrane Helix. *J. Comput. Phys.* **1999**, *151*, 358 – 387.

(43) Prakash, P.; Sankararamakrishnan, R. Force field dependence of phospholipid headgroup and acyl chain properties: Comparative molecular dynamics simulations of DMPC bilayers. *J. Comp. Chem.* **2010**, *31*, 266–277.

(44) Berger, O.; Edholm, O.; Jähnig, F. Molecular dynamics simulations of a fluid bilayer of dipalmitoylphosphatidylcholine at full hydration, constant pressure, and constant temperature. *Biophys. J.* **1997**, *72*, 2002 – 2013.

(45) Bechinger, B.; Seelig, J. Conformational changes of the phosphatidylcholine headgroup due to membrane dehydration. A 2H-NMR study. *Chem. Phys. Lipids* **1991**, *58*, 1 – 5.

(46) Ulrich, A.; Watts, A. Molecular response of the lipid headgroup to bilayer hydration monitored by 2H-NMR. *Biophys. J.* **1994**, *66*, 1441 – 1449.

(47) Dvinskikh, S. V.; Castro, V.; Sandstrom, D. Probing segmental order in lipid bilayers

at variable hydration levels by amplitude- and phase-modulated cross-polarization NMR. *Phys. Chem. Chem. Phys.* **2005**, *7*, 3255–3257.

(48) Brown, M. F.; Seelig, J. Influence of cholesterol on the polar region of phosphatidylcholine and phosphatidylethanolamine bilayers. *Biochemistry* **1978**, *17*, 381–384.

(49) Brown, M. F.; Seelig, J. Ion-induced changes in head group conformation of lecithin bilayers. *Nature* **1977**, *269*, 721–723.

(50) Akutsu, H.; Seelig, J. Interaction of metal ions with phosphatidylcholine bilayer membranes. *Biochemistry* **1981**, *20*, 7366–7373.

(51) Altenbach, C.; Seelig, J. Calcium binding to phosphatidylcholine bilayers as studied by deuterium magnetic resonance. Evidence for the formation of a calcium complex with two phospholipid molecules. *Biochemistry* **1984**, *23*, 3913–3920.

(52) Roux, M.; Bloom, M. Calcium, magnesium, lithium, sodium, and potassium distributions in the headgroup region of binary membranes of phosphatidylcholine and phosphatidylserine as seen by deuterium NMR. *Biochemistry* **1990**, *29*, 7077–7089.

(53) Roux, M.; Bloom, M. Calcium binding by phosphatidylserine headgroups. Deuterium {NMR} study. *Biophys. J.* **1991**, *60*, 38 – 44.

(54) Gally, H. U.; Niederberger, W.; Seelig, J. Conformation and motion of the choline head group in bilayers of dipalmitoyl-3-sn-phosphatidylcholine. *Biochemistry* **1975**, *14*, 3647–3652.

(55) Scherer, P. G.; Seelig, J. Electric charge effects on phospholipid headgroups. Phosphatidylcholine in mixtures with cationic and anionic amphiphiles. *Biochemistry* **1989**, *28*, 7720–7728.

(56) Browning, J. L.; Akutsu, H. Local anesthetics and divalent cations have the same effect

on the headgroups of phosphatidylcholine and phosphatidylethanolamine. *Biochim. Biophys. Acta* **1982**, *684*, 172 – 178.

(57) Kelusky, E. C.; Smith, I. C. The influence of local anesthetics on molecular organization in phosphatidylethanolamine membranes. *Mol. Pharmacol.* **1984**, *26*, 314–321.

(58) Roux, M.; Neumann, J. M.; Hodges, R. S.; Devaux, P. F.; Bloom, M. Conformational changes of phospholipid headgroups induced by a cationic integral membrane peptide as seen by deuterium magnetic resonance. *Biochemistry* **1989**, *28*, 2313–2321.

(59) Kuchinka, E.; Seelig, J. Interaction of melittin with phosphatidylcholine membranes. Binding isotherm and lipid head-group conformation. *Biochemistry* **1989**, *28*, 4216–4221.

(60) Catte, A.; Girych, M.; Javanainen, M.; Miettinen, M. S.; Monticelli, L.; Määttä, J.; Oganesyan, V. S.; Ollila, O. H. S. The electrometer concept and binding of cations to phospholipid bilayers. 2015; DOI: 10.5281/zenodo.32175.

(61) The NMRLipids project. 2015; `http://web.archive.org/web/20150414084452/http://nmrlipids.blogspot.fi`.

(62) Gowers, T.; Nielsen, M. Massively collaborative mathematics. *Nature* **2009**, *461*, 879–881.

(63) Ollila, O. H. S. Response of the hydrophilic part of lipid membranes to changing conditions - a critical comparison of simulations to experiments. 2013; `http://arxiv.org/abs/1309.2131v1`.

(64) The NMRLipids project, On credits. 2013; DOI: 10.6084/m9.figshare.1577577.

(65) ohsOllila,; markussmiettinen,; Hub,; mattijavanainen,; Retegan, M.; ClaireLoison,; lucamonticelli,; jsmaatta,; Fercho, nmrlipids.blogspot.fi: Submission to J. Phys. Chem. 2015.

(66) Seelig, J. Deuterium magnetic resonance: theory and application to lipid membranes. *Q. Rev. Biophys.* **1977**, *10*, 353–418.

(67) Hong, M.; Schmidt-Rohr, K.; Pines, A. NMR Measurement of Signs and Magnitudes of C-H Dipolar Couplings in Lecithin. *J. Am. Chem. Soc.* **1995**, *117*, 3310–3311.

(68) Gross, J. D.; Warschawski, D. E.; Griffin, R. G. Dipolar Recoupling in MAS NMR: A Probe for Segmental Order in Lipid Bilayers. *J. Am. Chem. Soc.* **1997**, *119*, 796–802.

(69) Dvinskikh, S. V.; Castro, V.; Sandstrom, D. Efficient solid-state NMR methods for measuring heteronuclear dipolar couplings in unoriented lipid membrane systems. *Phys. Chem. Chem. Phys.* **2005**, *7*, 607–613.

(70) The NMRLipids project, Accuracy of order parameter measurements. 2014; DOI: 10.6084/m9.figshare.1577576.

(71) The NMRLipids project, On the signs of the order parameters. 2014; DOI: 10.6084/m9.figshare.1577578.

(72) Engel, A. K.; Cowburn, D. The origin of multiple quadrupole couplings in the deuterium {NMR} spectra of the 2 chain of 1,2 dipalmitoyl-sn-glycero-3-phosphorylcholine. *FEBS Letters* **1981**, *126*, 169 – 171.

(73) Vogel, A.; Feller, S. Headgroup Conformations of Phospholipids from Molecular Dynamics Simulation: Sampling Challenges and Comparison to Experiment. *The Journal of Membrane Biology* **2012**, *245*, 23–28.

(74) Ollila, S.; Hyvönen, M. T.; Vattulainen, I. Polyunsaturation in Lipid Membranes: Dynamic Properties and Lateral Pressure Profiles. *J. Phys. Chem. B* **2007**, *111*, 3139–3150.

(75) Ferreira, T. M.; Ollila, O. H. S.; Pigliapochi, R.; Dabkowska, A. P.; Topgaard, D. Model-free estimation of the effective correlation time for CH bond reorientation in

amphiphilic bilayers: 1H13C solid-state NMR and MD simulations. *J. Chem. Phys.* **2015**, *142*, 044905.

(76) Hess, B.; Kutzner, C.; van der Spoel, D.; Lindahl, E. GROMACS 4: Algorithms for Highly Efficient, Load-Balanced, and Scalable Molecular Simulation. *J. Chem. Theory Comput.* **2008**, *4*, 435–447.

(77) Plimpton, S. Fast Parallel Algorithms for Short-Range Molecular Dynamics. *J. Comput. Phys.* **1995**, *117*, 1 – 19.

(78) Lyubartsev, A. P.; Laaksonen, A. M.DynaMix  a scalable portable parallel {MD} simulation package for arbitrary molecular mixtures. *Comp. Phys. Comm.* **2000**, *128*, 565 – 589.

(79) Phillips, J. C.; Braun, R.; Wang, W.; Gumbart, J.; Tajkhorshid, E.; Villa, E.; Chipot, C.; Skeel, R. D.; Kalé, L.; Schulten, K. Scalable molecular dynamics with NAMD. *J. Comput. Chem.* **2005**, *26*, 1781–1802.

(80) Gurtovenko, A. A.; Patra, M.; Karttunen, M.; Vattulainen, I. Cationic DMPC/DMTAP Lipid Bilayers: Molecular Dynamics Study. *Biophys. J.* **2004**, *86*, 3461 – 3472.

(81) Miettinen, M. S. Molecular dynamics simulation trajectory of a fully hydrated DMPC lipid bilayer. 2013; DOI: 10.6084/m9.figshare.829642.

(82) Miettinen, M. S.; Gurtovenko, A. A.; Vattulainen, I.; Karttunen, M. Ion Dynamics in Cationic Lipid Bilayer Systems in Saline Solutions. *J. Phys. Chem. B* **2009**, *113*, 9226–9234.

(83) Marrink, S.-J.; Berger, O.; Tieleman, P.; Jähnig, F. Adhesion Forces of Lipids in a Phospholipid Membrane Studied by Molecular Dynamics Simulations. *Biophys. J.* **1998**, *74*, 931 – 943.

(84) Määttä, J. DPPC_Berger. 2015; DOI: 10.5281/zenodo.13934.

(85) Ollila, O. H. S.; Ferreira, T.; Topgaard, D. MD simulation trajectory and related files for POPC bilayer (Berger model delivered by Tieleman, Gromacs 4.5). 2014; DOI: 10.5281/zenodo.13279.

(86) Ollila, O. H. S.; Miettinen, M. MD simulation trajectory and related files for DPPC bilayer (CHARMM36, Gromacs 4.5). 2015; DOI: 10.5281/zenodo.15549.

(87) Ollila, O. H. S.; Miettinen, M. MD simulation trajectory and related files for POPC bilayer (CHARMM36, Gromacs 4.5). 2015; DOI: 10.5281/zenodo.13944.

(88) Santuz, H. MD simulation trajectory and related files for POPC bilayer (CHARMM36, Gromacs 4.5). 2015; DOI: 10.5281/zenodo.14066.

(89) Kulig, W.; Pasenkiewicz-Gierula, M.; Róg, T. Cis and Trans Unsaturated Phosphatidylcholine Bilayers: A Molecular Dynamics Simulation Study. *Chem. Phys. Lipids* **2015**, *In Press, Accepted Manuscript, http://dx.doi.org/10.1016/j.chemphyslip.2015.07.002*.

(90) Javanainen, M. POPC @ 310K, model by Maciejewski and Rog. 2014; DOI: 10.5281/zenodo.13497.

(91) Javanainen, M. POPC/Cholesterol @ 310K. 0, 10, 40, 50 and 60 mol-cholesterol. Model by Maciejewski and Rog. 2015; DOI: 10.5281/zenodo.13877.

(92) Javanainen, M. POPC @ 310K, varying water-to-lipid ratio. Model by Maciejewski and Rog. 2014; DOI: 10.5281/zenodo.13498.

(93) Ollila, O. H. S.; Retegan, M. MD simulation trajectory and related files for DPPC bilayer (GAFFlipid, Gromacs 4.5). 2015; DOI: 10.5281/zenodo.15550.

(94) Ollila, O. H. S.; Retegan, M. MD simulation trajectory and related files for POPC bilayer (GAFFlipid, Gromacs 4.5). 2015; DOI: 10.5281/zenodo.13791.

(95) Dickson, C. J.; Madej, B. D.; Skjevik, . A.; Betz, R. M.; Teigen, K.; Gould, I. R.; Walker, R. C. Lipid14: The Amber Lipid Force Field. *J. Chem. Theory Comput.* **2014**, *10*, 865–879.

(96) Ollila, O. H. S.; Retegan, M. MD simulation trajectory and related files for POPC bilayer (Lipid14, Gromacs 4.5). 2014; DOI: 10.5281/zenodo.12767.

(97) Poger, D.; Van Gunsteren, W. F.; Mark, A. E. A new force field for simulating phosphatidylcholine bilayers. *J. Comput. Chem.* **2010**, *31*, 1117–1125.

(98) Fuchs, P. F. MD simulation trajectory and related files for DPPC bilayer in full hydration (Poger GROMOS53A6_L, Gromacs 4.0.7, PME, traj 1). 2015; DOI: 10.5281/zenodo.14594.

(99) Fuchs, P. F. MD simulation trajectory and related files for DPPC bilayer in full hydration (Poger GROMOS53A6_L, Gromacs 4.0.7, PME, traj 2). 2015; DOI: 10.5281/zenodo.14595.

(100) Jämbeck, J. P. M.; Lyubartsev, A. P. Derivation and Systematic Validation of a Refined All-Atom Force Field for Phosphatidylcholine Lipids. *J. Phys. Chem. B* **2012**, *116*, 3164–3179.

(101) Määttä, J. DPPC_Slipids. 2014; DOI: 10.5281/zenodo.13287.

(102) Jämbeck, J. P. M.; Lyubartsev, A. P. An Extension and Further Validation of an All-Atomistic Force Field for Biological Membranes. *J. Chem. Theory Comput.* **2012**, *8*, 2938–2948.

(103) Javanainen, M. POPC @ 310K, Slipids force field. 2015; DOI: 10.5281/zenodo.13887.

(104) Kukol, A. Lipid Models for United-Atom Molecular Dynamics Simulations of Proteins. *J. Chem. Theory Comput.* **2009**, *5*, 615–626.

(105) Javanainen, M. POPC @ 298K, Model by Kukol. 2014; DOI: 10.5281/zenodo.13393.

(106) Chiu, S.-W.; Pandit, S. A.; Scott, H. L.; Jakobsson, E. An Improved United Atom Force Field for Simulation of Mixed Lipid Bilayers. *J. Phys. Chem. B* **2009**, *113*, 2748–2763.

(107) Ollila, O. H. S. MD simulation trajectory and related files for POPC bilayer (Chiu et al. Gromos version, Gromacs 4.5). 2015; DOI: 10.5281/zenodo.15548.

(108) Lyubartsev, A. MD simulation trajectory and related files for DMPC bilayer, Högberg et al, J.Comp.Chem., 29, 2359 (2008). 2015; DOI: 10.5281/zenodo.16195.

(109) Rabinovich, A. L.; Lyubartsev, A. P. Bond orientation properties in lipid molecules of membranes: molecular dynamics simulations. *J. Phys. Conf. Ser.* **2014**, *510*, 012022.

(110) Lyubartsev, A. MD simulation trajectory and related files for POPC bilayer, Högberg et al parameters (J.Comp.Chem., 29, 2359 (2008)). 2015; DOI: 10.5281/zenodo.16724.

(111) Ulmschneider, J. P.; Ulmschneider, M. B. United Atom Lipid Parameters for Combination with the Optimized Potentials for Liquid Simulations All-Atom Force Field. *J. Chem. Theory Comput.* **2009**, *5*, 1803–1813.

(112) Javanainen, M. POPC @ 310K, Model by Ulmschneider and Ulmschneider. 2014; DOI: 10.5281/zenodo.13392.

(113) Tjörnhammar, R.; Edholm, O. Reparameterized United Atom Model for Molecular Dynamics Simulations of Gel and Fluid Phosphatidylcholine Bilayers. *J. Chem. Theory Comput.* **2014**, *10*, 5706–5715.

(114) Javanainen, M. DPPC @ 323K, new FF by Tjörnhammar and Edholm. 2014; DOI: 10.5281/zenodo.12743.

(115) Henin, J.; Shinoda, W.; Klein, M. L. United-Atom Acyl Chains for CHARMM Phospholipids. *J. Phys. Chem. B* **2008**, *112*, 7008–7015.

(116) Botan, A. DLPC@ 323K, CHARMM36UA force field. 2015; DOI: 10.5281/zenodo.13821.

(117) Lee, S.; Tran, A.; Allsopp, M.; Lim, J. B.; Henin, J.; Klauda, J. B. CHARMM36 United Atom Chain Model for Lipids and Surfactants. *J. Phys. Chem. B* **2014**, *118*, 547–556.

(118) Loison, C. Hydrated DPPC, MD simulation trajectory and related files for UA charmm36 model by Lee et al 2014. 2015; DOI: 10.5281/zenodo.17004.

(119) Ollila, O. H. S. MD simulation trajectory and related files for POPC bilayer in low hydration (Berger model delivered by Tieleman, Gromacs 4.5). 2015; DOI: 10.5281/zenodo.13814.

(120) Kanduc, M.; Schneck, E.; Netz, R. R. Hydration Interaction between Phospholipid Membranes: Insight into Different Measurement Ensembles from Atomistic Molecular Dynamics Simulations. *Langmuir* **2013**, *29*, 9126–9137.

(121) Kanduc, M. MD trajectory for DLPC bilayer (Berger, Gromacs 4.5.4), nw=28 w/l. 2015; DOI: 10.5281/zenodo.16287.

(122) Kanduc, M. MD trajectory for DLPC bilayer (Berger, Gromacs 4.5.4), nw=24 w/l. 2015; DOI: 10.5281/zenodo.16289.

(123) Kanduc, M. MD trajectory for DLPC bilayer (Berger, Gromacs 4.5.4), nw=20 w/l. 2015; DOI: 10.5281/zenodo.16291.

(124) Kanduc, M. MD trajectory for DLPC bilayer (Berger, Gromacs 4.5.4), nw=16 w/l. 2015; DOI: 10.5281/zenodo.16292.

(125) Kanduc, M. MD trajectory for DLPC bilayer (Berger, Gromacs 4.5.4), nw=28 w/l. 2015; DOI: 10.5281/zenodo.16293.

(126) Kanduc, M. MD trajectory for DLPC bilayer (Berger, Gromacs 4.5.4), nw=8 w/l. 2015; DOI: 10.5281/zenodo.16294.

(127) Kanduc, M. MD trajectory for DLPC bilayer (Berger, Gromacs 4.5.4), nw=4 w/l. 2015; DOI: 10.5281/zenodo.16295.

(128) Ollila, O. H. S.; Miettinen, M. MD simulation trajectory and related files for POPC bilayer in medium low hydration (CHARMM36, Gromacs 4.5). 2015; DOI: 10.5281/zenodo.13946.

(129) Ollila, O. H. S.; Miettinen, M. MD simulation trajectory and related files for POPC bilayer in low hydration (CHARMM36, Gromacs 4.5). 2015; DOI: 10.5281/zenodo.13945.

(130) Ollila, O. H. S. MD simulation trajectory and related files for POPC bilayer in low hydration (GAFFlipid, Gromacs 4.5). 2015; DOI: 10.5281/zenodo.13853.

(131) Höltje, M.; Förster, T.; Brandt, B.; Engels, T.; von Rybinski, W.; Höltje, H.-D. Molecular dynamics simulations of stratum corneum lipid models: fatty acids and cholesterol. *Biochim. Biophys. Acta* **2001**, *1511*, 156 – 167.

(132) Ollila, O. H. S.; Ferreira, T.; Topgaard, D. MD simulation trajectory and related files for POPC/cholesterol (7 mol%) bilayer (Berger model delivered by Tieleman, modified Höltje, Gromacs 4.5). 2014; DOI: 10.5281/zenodo.13282.

(133) Ollila, O. H. S.; Ferreira, T.; Topgaard, D. MD simulation trajectory and related files for POPC/cholesterol (15 mol%) bilayer (Berger model delivered by Tieleman, modified Höltje, Gromacs 4.5). 2014; DOI: 10.5281/zenodo.13281.

(134) Ollila, O. H. S.; Ferreira, T.; Topgaard, D. MD simulation trajectory and related files for POPC/cholesterol (34 mol%) bilayer (Berger model delivered by Tieleman, modified Höltje, Gromacs 4.5). 2014; DOI: 10.5281/zenodo.13283.

(135) Ollila, O. H. S.; Ferreira, T.; Topgaard, D. MD simulation trajectory and related files for POPC/cholesterol (50 mol%) bilayer (Berger model delivered by Tieleman, modified Höltje, Gromacs 4.5). 2014; DOI: 10.5281/zenodo.13285.

(136) Ollila, O. H. S.; Ferreira, T.; Topgaard, D. MD simulation trajectory and related files for POPC/cholesterol (60 mol%) bilayer (Berger model delivered by Tieleman, modified Höltje, Gromacs 4.5). 2014; DOI: 10.5281/zenodo.13286.

(137) Lim, J. B.; Rogaski, B.; Klauda, J. B. Update of the Cholesterol Force Field Parameters in CHARMM. *J. Phys. Chem. B* **2012**, *116*, 203–210.

(138) Fernando, F.-R. POPC_Glycerol_CHARMM36_0-10-15-20-25-35-50%CHOL. 2015; Because of the system size, the files ONLY contain the coordinates of Glycerol saved every 10ps, this is the real contribution to the nmrlipids project.

(139) Santuz, H. MD simulation trajectory for POPC/20% Chol bilayer (CHARMM36, Gromacs 4.5). 2015; DOI: 10.5281/zenodo.14067.

(140) Santuz, H. MD simulation trajectory for POPC/50% Chol bilayer (CHARMM36, Gromacs 4.5). 2015; DOI: 10.5281/zenodo.14068.

(141) Warschawski, D.; Devaux, P. Order parameters of unsaturated phospholipids in membranes and the effect of cholesterol: a 1H13C solid-state NMR study at natural abundance. *Eur. Biophys. J.* **2005**, *34*, 987–996.

(142) Mashl, R. J.; Scott, H. L.; Subramaniam, S.; Jakobsson, E. Molecular Simulation of Dioleoylphosphatidylcholine Lipid Bilayers at Differing Levels of Hydration. *Biophys. J.* **2001**, *81*, 3005 – 3015.

(143) Pertsin, A.; Platonov, D.; Grunze, M. Direct computer simulation of water-mediated force between supported phospholipid membranes. *J. Chem. Phys.* **2005**, *122*, 244708.

(144) Pertsin, A.; Platonov, D.; Grunze, M. Origin of Short-Range Repulsion between Hydrated Phospholipid Bilayers: A Computer Simulation Study. *Langmuir* **2007**, *23*, 1388–1393.

(145) Eun, C.; Berkowitz, M. L. Origin of the Hydration Force: Water-Mediated Interaction between Two Hydrophilic Plates. *J. Phys. Chem. B* **2009**, *113*, 13222–13228.

(146) Eun, C.; Berkowitz, M. L. Thermodynamic and Hydrogen-Bonding Analyses of the Interaction between Model Lipid Bilayers. *J. Phys. Chem. B* **2010**, *114*, 3013–3019.

(147) Schneck, E.; Sedlmeier, F.; Netz, R. R. Hydration repulsion between biomembranes results from an interplay of dehydration and depolarization. *Proc. Natl. Acad. Sci. USA* **2012**, *109*, 14405–14409.

(148) Israelachvili, J. N. *Intermolecular and Surface Forces*; Academic Press: London, 1985.

(149) Israelachvili, J. N.; Wennerström, H. Role of hydration and water structure in biological and colloidal interactions. *Nature* **1996**, *379*, 219 – 225.

(150) Sparr, E.; Wennerström, H. Interlamellar forces and the thermodynamic characterization of lamellar phospholipid systems. *Curr. Opin. Colloid Interf. Science* **2011**, *16*, 561 – 567.

(151) Simons, K.; Vaz, W. L. Model Systems, Lipid Rafts, And Cell Membranes. *Ann. Rev. Biophys. Biomol. Struct.* **2004**, *33*, 269–295.

(152) Somerharju, P.; Virtanen, J. A.; Cheng, K. H.; Hermansson, M. The superlattice model of lateral organization of membranes and its implications on membrane lipid homeostasis. *Biochim. Biophys. Acta - Biomembranes* **2009**, *1788*, 12 – 23.

(153) Huang, J.; Feigenson, G. W. A Microscopic Interaction Model of Maximum Solubility of Cholesterol in Lipid Bilayers. *Biophys. J.* **1999**, *76*, 2142 – 2157.

(154) Zhu, Q.; Cheng, K. H.; Vaughn, M. W. Molecular Dynamics Studies of the Molecular Structure and Interactions of Cholesterol Superlattices and Random Domains in an Unsaturated Phosphatidylcholine Bilayer Membrane. *J. Phys. Chem. B* **2007**, *111*, 11021–11031.

(155) Rog, T.; Pasenkiewicz-Gierula, M.; Vattulainen, I.; Karttunen, M. Ordering effects of cholesterol and its analogues. *Biochim. Biophys. Acta* **2009**, *1788*, 97 – 121.

(156) Alwarawrah, M.; Dai, J.; Huang, J. Modification of Lipid Bilayer Structure by Diacylglycerol: A Comparative Study of Diacylglycerol and Cholesterol. *J. Chem. Theor. Comput.* **2012**, *8*, 749–758.

(157) Marsh, D. Liquid-ordered phases induced by cholesterol: A compendium of binary phase diagrams. *Biochim. Biophys. Acta* **2010**, *1798*, 688 – 699.

(158) Ghosh, R.; Seelig, J. The interaction of cholesterol with bilayers of phosphatidylethanolamine. *Biochim. Biophys. Acta* **1982**, *691*, 151 – 160.

(159) Ferreira, T. M.; Topgaard, D.; Ollila, O. H. S. O. Molecular Conformation and Bilayer Pores in a Nonionic Surfactant Lamellar Phase Studied with 1H13C Solid-State NMR and Molecular Dynamics Simulations. *Langmuir* **2014**, *30*, 461–469.

# Graphical TOC Entry